Ultramicroscopy 121 (2012) 31–37

Contents lists available at SciVerse ScienceDirect

Ultramicroscopy

journal homepage: www.elsevier.com/locate/ultramic

Assessment of lower-voltage TEM performance using 3D Fourier transform of through-focus series

Koji Kimoto [a,c,*], Keiji Kurashima [a], Takuro Nagai [a], Megumi Ohwada [a], Kazuo Ishizuka [b,a]

[a] National Institute for Materials Science, 1-1 Namiki, Tsukuba, Ibaraki 305-0044, Japan
[b] HREM Research Inc., 14-48 Matsukazedai, Higashimatsuyama, Saitama 355-0055, Japan
[c] Research Acceleration Program, Japan Science and Technology Agency, Japan

A R T I C L E I N F O

Article history:
Received 26 May 2011
Received in revised form
2 June 2012
Accepted 9 June 2012
Available online 26 June 2012

Keywords:
High-resolution transmission electron microscopy
Low acceleration voltage
Spherical aberration corrector
Information limit
Young fringe
Monochromator

A B S T R A C T

We assess the imaging performance of a transmission electron microscopy (TEM) system operated at a relatively low acceleration voltage using the three-dimensional (3D) Fourier transform of through-focus images. Although a single diffractogram and the Thon diagram cannot distinguish between the linear and non-linear TEM imaging terms, the 3D Fourier transform allows us to evaluate linear imaging terms, resulting in a conclusive assessment of TEM performance. Using this method, information transfer up to 98 pm is demonstrated for an 80 kV TEM system equipped with a spherical aberration corrector and a monochromator. We also revisit the Young fringe method in the light of the 3D Fourier transform, and have found a considerable amount of non-linear terms in Young fringes at 80 kV even from a typical standard specimen, such as an amorphous Ge thin film.

1. Introduction

Lower-voltage transmission electron microscopy (TEM) has recently attracted much attention, because it can reduce knock-on damage and enhance image contrast [1,2]. At a lower acceleration voltage, not only the 3rd-order spherical aberration C_3, but also other aberrations become critical for achieving high spatial resolution. One of the critical aberrations is the six-fold astigmatism of hexapole-based aberration correctors, and it has been minimized only recently [3,4]. The other critical factor is chromatic aberration. In contrast to incoherent STEM imaging, conventional TEM imaging is substantially affected by chromatic aberration, which reduces the information limit by a defocus spread. Since the defocus spread mainly depends on the chromatic aberration of image-forming lenses and the energy spread of an electron source, one solution is a chromatic aberration corrector [5–7], and the other alternative approach is a monochromator [8–10].

TEM spatial resolution is often evaluated using the Young fringe method, in which the diffractogram of a double-exposure image with a given image shift is analyzed [11]. The Young fringe method is effective to distinguish image signals from random noises, and the stability of an electron microscope can be evaluated. Several authors, however, pointed out the limitation of the Young fringe method in estimating the information limit [12–14]. In the weak-scattering approximation, a TEM image is composed of interference fringes between a strong transmitted wave and weak diffracted waves (the linear term), and weak interference fringes between diffracted waves (non-linear terms) are considered to be negligible. An inherent TEM performance should be evaluated by the linear term, because the linear term is proportional to the potential distribution of the specimen. The Young fringe method, however, could not discriminate between linear and non-linear terms. In the case of lower-voltage TEM, a typical standard specimen might no longer be a weak-scattering object because of the strong interaction between a slow electron and materials, and the TEM images might be affected significantly by non-linear terms. Therefore, the assessment of lower-voltage microscopes involves difficulty in evaluating the inherent imaging performance. An information limit of TEM is often discussed on the basis of temporal and/or spatial incoherent envelope functions, which determine the upper limit of information transfer at particular imaging conditions [15]. Currently, in most cases a temporal (chromatic) incoherent envelope function determines the upper limit of information transfer, and a novel way to estimate the temporal envelope function has been devised [12]. In the case of an advanced corrected microscope equipped with a

* Corresponding author at: National Institute for Materials Science, 1-1 Namiki, Tsukuba, Ibaraki 305-0044, Japan. Tel.: +81 29 860 4402.
E-mail address: kimoto.koji@nims.go.jp (K. Kimoto).

0304-3991/$ - see front matter © 2012 Elsevier B.V. All rights reserved.
http://dx.doi.org/10.1016/j.ultramic.2012.06.012

monochromator or a chromatic aberration corrector, its performance may not simply be limited by the temporal incoherence.

Here, we assess the limit of information transfer of lower-voltage TEM using the three-dimensional (3D) Fourier transform of through-focus images. Using this method, information transfer is evaluated for an 80 kV transmission electron microscope equipped with a C_3-corrector and a monochromator. We also revisit the Young fringe method, which is still often demonstrated for advanced microscopy, in the light of the 3D Fourier transform method.

2. Methods

2.1. Electron microscopy

We used a transmission electron microscope (FEI, Titan^3) equipped with a monochromator, a spherical aberration corrector for image forming (CEOS, CETCOR), a charge-coupled-device (CCD) camera (Gatan, Inc., UltraScan) and an energy filter (Gatan, Inc., Quantum) operated at an acceleration voltage E_0 of 80 kV. The full width at half maximum of the energy spread of a high-brightness Schottky emitter (FEI, X-FEG) was 0.93 eV, which was reduced to 0.10 eV by the monochromator. In the monochromated TEM imaging, a specimen was illuminated by energy-dispersed incident electrons, which is the so-called rainbow illumination [9]. The TEM defocus modulation Δz per acceleration voltage change ΔE was evaluated to be 18.8 nm/V. The chromatic aberration coefficient C_c of the image-forming lenses, including the objective postfield lens and the spherical aberration corrector, was then evaluated to be 1.50 mm using $\Delta z = C_c(\Delta E/E_0)$. Thus, the nominal defocus spreads due to the energy spread of the electron source were approximately 17.5 nm and 1.9 nm for the non-monochromated and monochromated experiments, respectively. The 3rd-order spherical aberration was corrected to less than 1 μm. A cubic enclosure of the microscope almost suppressed environmental disturbance, and furthermore, the microscope was installed on an active vibration-isolation system (Tokkyokiki Corporation) in a room with a panel-cooling air conditioning system (Nihon Spindle Manufacturing Co., Ltd.). Thus, a high specimen stage stability of less than 0.2 nm/min was routinely realized.

2.2. Data acquisition and analyses

Through-focus TEM images were acquired and analyzed using in-house scripts of DigitalMicrograph (Gatan, Inc.) [16]. While the defocus was controlled by the script, the accurate defocus step was recalibrated by analyzing an Ewald sphere curvature in the 3D Fourier transform of the through-focus images (see the following section). Some through-focus series of 160 images were acquired with a focus step of 1.37 nm around the minimum-contrast defocus. The exposure time for each image was 0.5 s, and the total acquisition time was about 10 min. Here, two images were acquired at each defocus for the Young fringe method as described in Section 4.4. TEM images with 1024×1024 pixels were acquired using the CDD camera after 2×2 binning. The single pixel size of the acquired images was 34.8 pm on the specimen, and thus the corresponding Nyquist frequency was 14.4 nm^{-1}. The specimen drifts during the through-focus acquisition were corrected after the experiment using cross correlation. The TEM specimen was an amorphous Ge thin film with Au particles with diameters of several nanometers (JEOL Datum Ltd.). The Ge film thickness was evaluated to be about 7 nm (0.14 times the total inelastic mean free path) using electron energy-loss spectroscopy [17].

3. Theoretical background

Electron microscopic techniques that use plural TEM images have been studied by several authors since the 70s, as reviewed by Saxton [18]. Among them, the defocus-image modulation processing [19–21] and the paraboloid method [22–24] have involved 3D Fourier transform of through-focus images in conjunction with 2D exit wave reconstruction using the 3D data set. The theoretical basis of 3D Fourier transform of through-focus images has already been given in these previous studies. We apply the 3D Fourier transform to the assessment of lower-voltage TEM, and this section briefly gives the outline of the theoretical background.

Fig. 1 schematically shows the variations of 3D data processed in this study. Acquired through-focus TEM images are stacked as a function of the defocus z after drift correction, and a 3D data set I_{xyz} is formed (Fig. 1(a)). Then, each TEM image is converted to its 2D Fourier transform, resulting in the stack of the 2D Fourier transforms $\boldsymbol{I}_{uvz}$ (Fig. 1(b)), where (x,y,z) and (u,v,w) are coordinates in real and reciprocal spaces, respectively. If the specimen corresponds to a weak-phase object, 2D Fourier transform of each image taken at a defocus of z may be given by

$$\boldsymbol{I}_{uvz} = \boldsymbol{I}(\boldsymbol{g};z) = \delta(\boldsymbol{g}) - 2\Phi(\boldsymbol{g})A(\boldsymbol{g})\sin\chi(\boldsymbol{g};z)K_t(\boldsymbol{g})K_s(\boldsymbol{g};z) + \text{non-linear terms} \quad (1)$$

here, $\Phi(\boldsymbol{g})$ represents the Fourier transform of the wave function at an exit specimen surface, $A(\boldsymbol{g})$ the aperture function, $\chi(\boldsymbol{g};z)$ the wave aberration function, $K_t(\boldsymbol{g})$ the temporal envelope function and $K_s(\boldsymbol{g};z)$ the spatial envelope function, where $\boldsymbol{g} = (u,v)$ is a scattering vector. The wave aberration may be decomposed into a

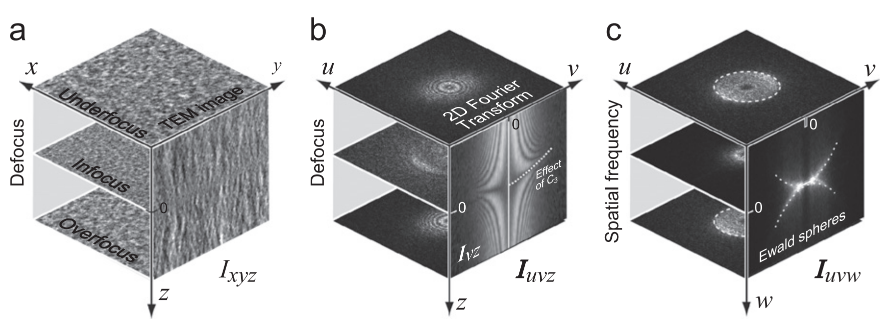

Fig. 1. Schematics of (a) through-focus TEM images I_{xyz}, (b) stack of 2D Fourier transforms $\boldsymbol{I}_{uvz}$, and (c) 3D Fourier transform of the through-focus images $\boldsymbol{I}_{uvw}$. Since $\boldsymbol{I}_{uvz}$ and $\boldsymbol{I}_{uvw}$ are complex, their moduli are shown in gray scale. The cross section $\boldsymbol{I}_{vz}$ is similar to the Thon diagram. Two Ewald spheres attached at the origin are observed in the 3D Fourier space I_{uvw}. Inset figures are obtained using a conventional 300 kV TEM system; therefore, we observe an asymmetric pattern in $\boldsymbol{I}_{vz}$ due to the 3rd-order spherical aberration C_3, as indicated by a dotted line in (b). Through-focus images were acquired by changing the acceleration voltage. Cross sections $\boldsymbol{I}_{vz}$ of C_3-corrected TEM are given in Fig. 3.